

CHARACTERIZATION OF AMORPHOUS $\text{Se}_{1-x}\text{Bi}_x$ ($x = 0.05$ at) COEVAPORATED THIN FILMS (*)

A. MUÑOZ, J. LEAL, A. CONDE, R. MÁRQUEZ

Departamento de Óptica y Sección de Física del Centro Coordinado del C.S.I.C.
Universidad de Sevilla. Spain.

(Received 5 January 1982)

ABSTRACT—Thermal evolution of amorphous $\text{Se}_{1-x}\text{Bi}_x$ ($x = 0.05$ at) coevaporated thin films has been characterized by electrical resistivity measurements and electron microscopy observations. Optical measurements on amorphous and crystallized films have been performed by ellipsometric methods.

1 — INTRODUCTION

The electronic properties of amorphous chalcogenide semiconductors can be modified or controlled by addition of some impurities; the effects of various kinds of foreign atoms on electrical conductivity, optical absorption, etc., have been extensively studied [1].

Bi-doped chalcogenides exhibit a striking feature: they show n-type conduction [2], [3] as opposed to the more common p-type conduction observed in chalcogenide semiconductors.

In this paper some initial results on the $\text{Se}_{1-x}\text{Bi}_x$ system ($x = 0.05$ at.) relative to crystallization and optical properties are reported. The aim of the work is to study possible differences between coevaporated thin films and the melt-quenched material of the same composition.

2 — EXPERIMENTAL

Thin films of $\text{Se}_{1-x}\text{Bi}_x$ were prepared by vacuum thermal evaporation ($\sim 10^{-4}$ Pa) of high-purity selenium and bismuth from two separate alumina crucibles. Glass and alumina substrates were used and kept during deposition at a temperature of ~ 170 K by liquid nitrogen refrigeration.

(*) Presented at the VII Iberoamerican Congress of Crystallography (21-26 September 1981, Coimbra, Portugal).

The film composition could be varied simply by controlling the crucible temperatures and for this work a value of $x \approx 0.5$ % at was selected. Composition and thickness of films were monitored during evaporation by a quartz oscillator device and the evaporation rate was 1.5 nm s^{-1} approximately.

For *in situ* electrical measurements films of thickness in the range between 50 and 500 nm were deposited onto alumina substrates in which Au electrical contacts had been evaporated previously. Electrical measurements were performed on films inside the evaporation chamber after concluding the film formation and a Keithley 602 electrometer was used.

Films for electron microscopy observation and optical measurements were deposited onto glass substrates and a higher thickness (~ 1500 nm) was used in the last case. Ellipsometric measurements were carried out on a classical device (Fig. 1) using a iodine lamp, a holographic grating monochromator and a quarter-wave plate for the Na wavelength λ of 589 nm. The measurements were made by null setting the polarizer and the analyser, which gave two characteristic parameters: Δ defined as the phase angle change, and Ψ defined as the arctangent of the amplitude ratio change [4]. In such measurements we could have two experimental parameters but there are three unknowns which are the refractive index n , the extinction coefficient k and the film thickness d . However, for films thicker than $1 \mu\text{m}$ the effect of the reflection at the substrate surface is negligible and the film thickness can be considered as infinite for short wavelengths.

In this work, the shortest and longest wavelengths used were 300 nm and 750 nm respectively owing to restrictions

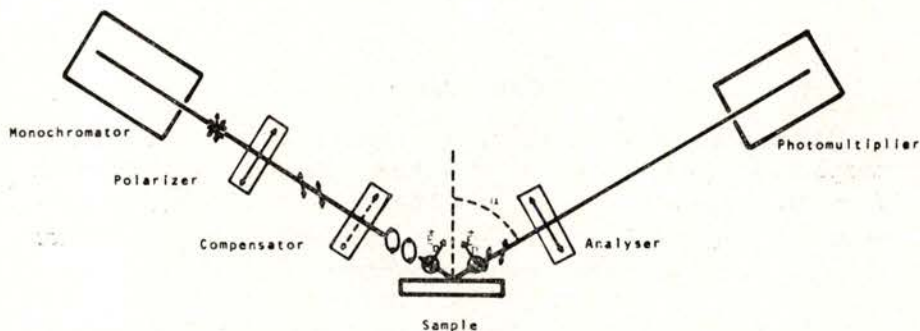


Fig. 1 — A schematic drawing of ellipsometric device.

imposed by the quality of the optical elements of the ellipsometric device. All measurements were performed at ~ 300 K in a dark room.

3 — RESULTS

3.1 — Electrical resistivity

Thermal evolution of electrical resistivity of films was studied between the deposition temperature (~ 170 K) and 400 K at a heating rate of 4 K min^{-1} approximately. For thicknesses in the explored range (50 to 500 nm) the ρ vs T curves exhibit the same qualitative features and Fig. 2 shows the temperature variation of electrical resistivity for a film of 80 nm thickness.

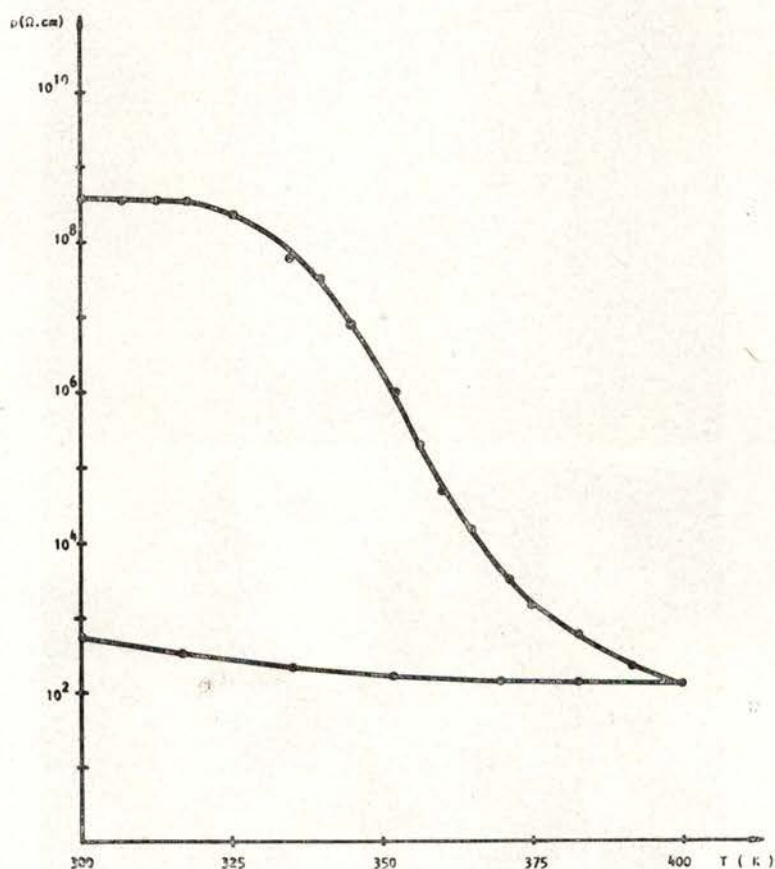


Fig. 2—Temperature dependence of electrical resistivity for a 80 nm thick film.

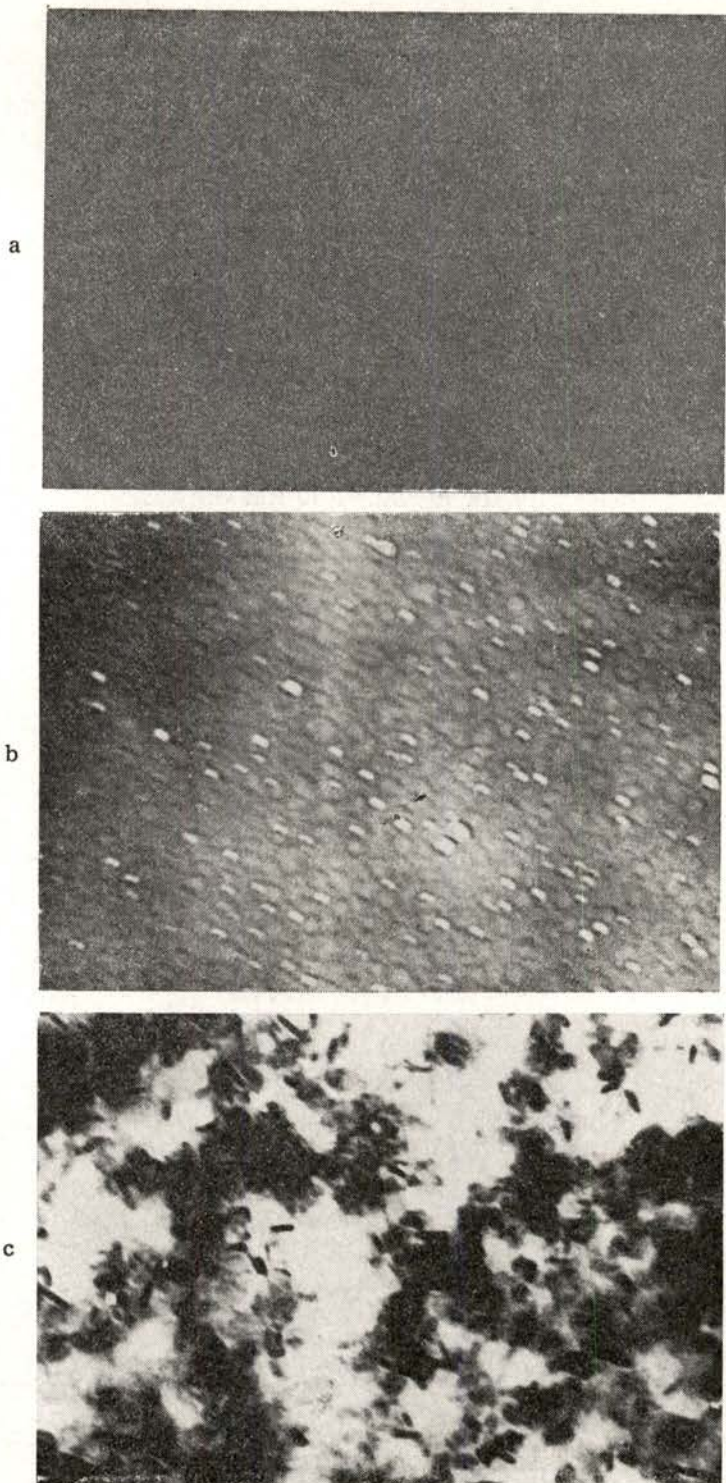
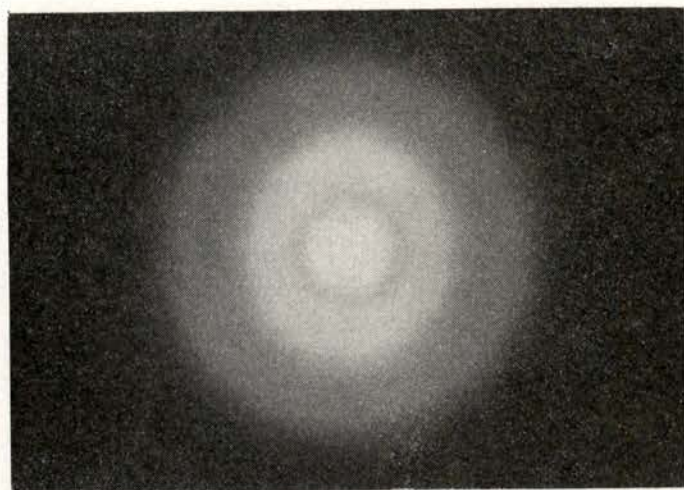
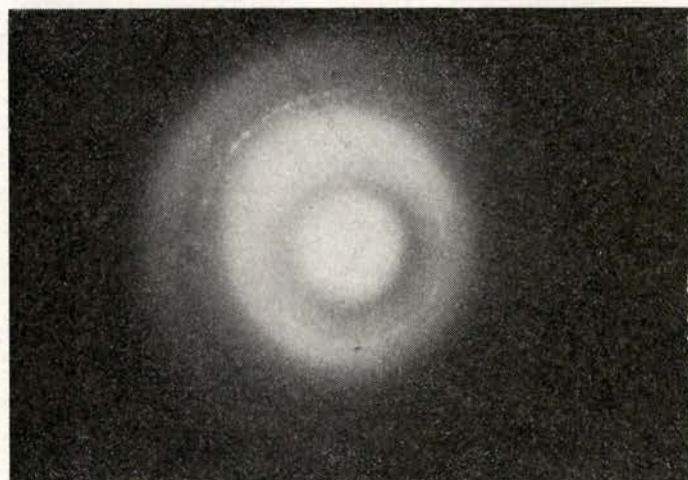


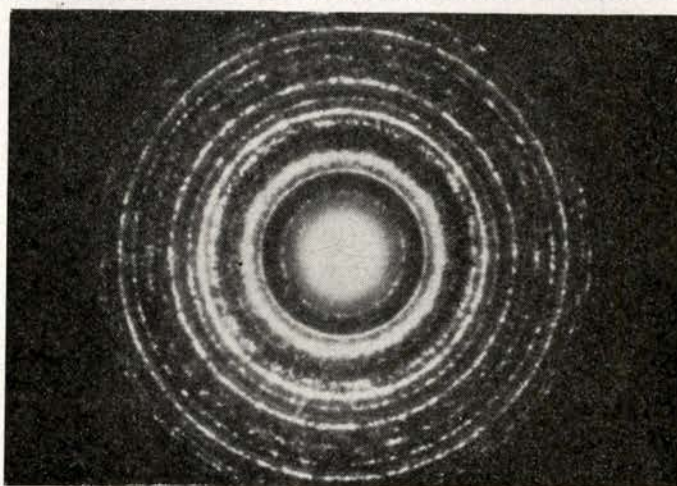
Fig. 3— Electron micrographs (x 110,000): a) amorphous film, b) intermediate stage of crystallization process and c) crystallized film.



a



b



c

Fig. 3 — Selected area diffraction patterns: a) amorphous film, b) intermediate stage of crystallization process and c) crystallized film.

As observed, the main feature in the ρ vs T curve is an abrupt fall of a few orders of magnitude around 350 K that we associate with the amorphous-crystal transformation. This agrees with the crystallization temperature $T_c \approx 360$ K [5] determined by calorimetric methods (DSC) for quenched material of the same composition. The irreversible character in the resistivity change is shown clearly in a subsequent cooling process.

3.2 — Electron microscopy

The amorphous character of the films has been proved by electron diffraction. The samples were observed in an electron microscope (100 KeV) using a cooling holder and defocussing the incident beam to prevent instantaneous crystallization. Fig. 3 shows electron micrographs and selected area diffraction patterns of three stages of thermal evolution inside the microscope. Fig. 3.a corresponds to the initial stage and reveals the non-crystalline character through the structureless features of the micrograph and the broadened haloes exhibited by the diffraction pattern. Fig. 3.b shows an intermediate stage of amorphous-crystal transformation as indicated by the grain structure in the micrograph and the rings observed in the diffraction pattern; finally, in Fig. 3.c the crystallization process is completed.

From the intensity of the amorphous diffraction pattern, measured with a Joyce microdensitometer, a first approximation to the structure factor (Fig. 4) has been obtained. The method proposed by Nabitovich *et al.* [6] has been used to eliminate the background intensity and estimate the normalization factor. Features of this structure factor are similar to those reported for amorphous selenium and quantitative differences among them are at first difficult to see.

3.3 — Optical measurements

The complex refractive index is defined as $n^* = n - ik$ where the real part is the refractive index and the imaginary part is the extinction coefficient. These constants can be derived [7] from the measured values of Δ and Ψ .

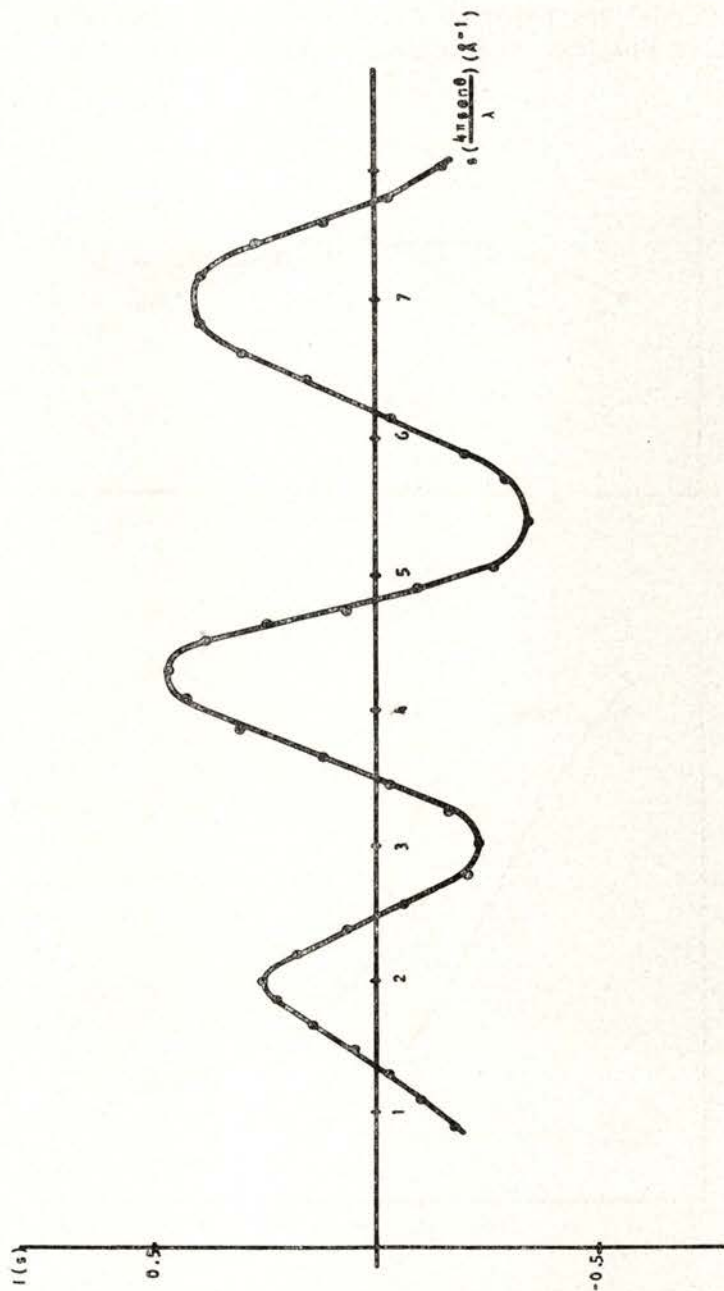


Fig. 4 — A first approximation to the structure factor.

The values of n and k as a function of wavelength of the incident light are shown in Fig. 5 for the amorphous films and after crystallization by annealing at 350 K during 24 h.

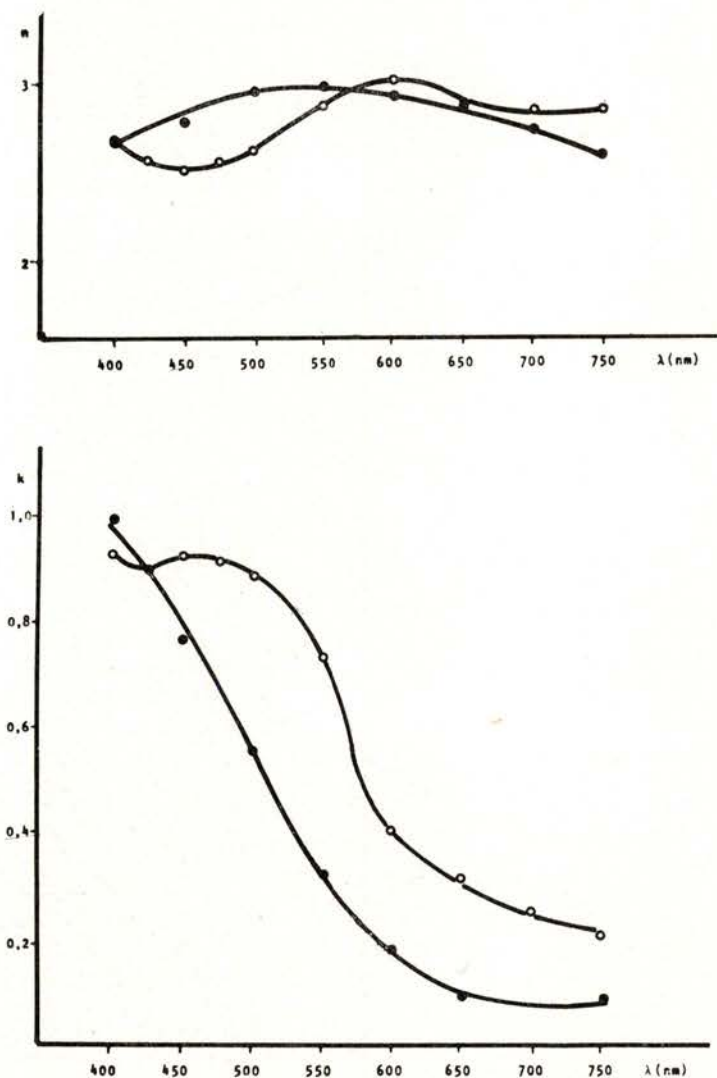


Fig. 5 — Complex refractive index as a function of wavelength for amorphous (●) and crystallized (○) films: a) refractive index, and b) extinction coefficient.

The real part ϵ' and the imaginary part ϵ'' of the complex dielectric constant can be calculated from the complex refractive index by

$$\begin{aligned}\epsilon' &= n^2 - k^2 \\ \epsilon'' &= 2nk\end{aligned}$$

and results derived from the data given in Fig. 5 are shown in Fig. 6. The features observed in the ϵ'' curves are analogous to

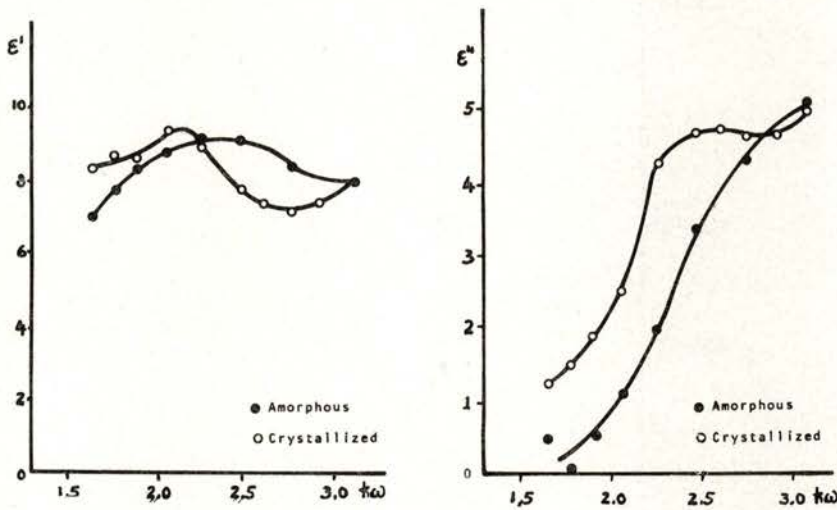


Fig. 6 — Complex dielectric constant as a function of incident photon energy, for amorphous and crystallized films: a) real part, and b) imaginary part.

those reported for amorphous selenium [1] and so the peak at ~ 2.5 eV shown for the crystal films is lost in the amorphous case.

The absorption coefficient α can be related to the extinction coefficient k by

$$\alpha = 4\pi k/\lambda$$

and Fig. 7 shows the values of the absorption coefficient calculated from the data given in Fig. 5.

For amorphous films, values of the absorption coefficient above the exponential edge fit very well the relation [8]:

$$\alpha \hbar \omega = A (\hbar \omega - E_{opt})^2$$

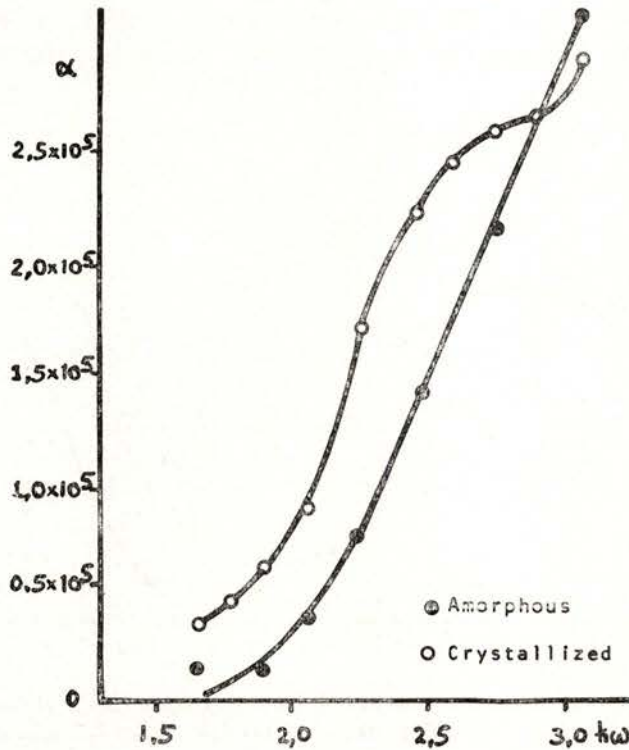


Fig. 7 — Absorption coefficient as a function of exciting photon energy for amorphous and crystallized films.

where E_{opt} is the optical band gap and A is a constant, as can be observed in Fig. 8. Values obtained from a least-squares fit are $E_{opt} = 1.63$ eV and $A = 6.8 \times 10^7$ m⁻¹ eV⁻¹ (linear regression coefficient $r = 0.999$). The computed value of the A constant is in good agreement with those predicted theoretically [1], [8]. For the crystallized films a worse fit is found: $E_{opt} = 1.41$ eV

and $A = 6.9 \times 10^7 \text{ m}^{-1} \text{ eV}^{-1}$ ($r = 0.892$); but a more satisfactory agreement is obtained in this case using the relation

$$\alpha \hbar \omega = A (\hbar \omega - E_{opt})$$

proposed [1] for amorphous selenium. A more detailed study is necessary to elucidate this point.

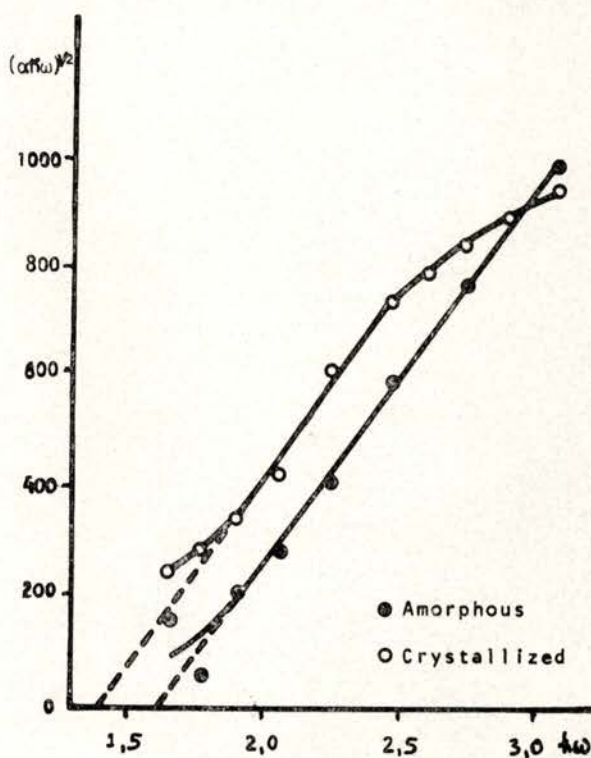


Fig. 8 — Values of $(\alpha \hbar \omega)^{1/2}$ as a function of exciting photon energy for amorphous and crystallized films.

REFERENCES

- [1] MOTT, N. F., DAVIS, E. A., *Electronic Processes in Non Crystalline Materials* (2nd ed.). Clarendon, p. 517 (1979).
- [2] HENKELS, H. W., MACZUK, J., *Phys. Rev.*, **24**, 1056 (1953).

A. MUÑOZ *et al.* — Amorphous $Se_{1-x}Bi_x$ ($x = 0.05$ at) coevaporated thin films

- [3] TOHGE, N., MINAMI, T., TANAKA, M. *J. Non Crystal. Solids*, **37**, 23 (1980); *J. Appl. Phys.*, **51**, 1048 (1980).
- [4] ARCHER, R. J. in the *Symposium on the Ellipsometer and its Use in the Measurements of Surfaces and Thin Films*. Natl. Bureau Stand. Washington D. C. (1963) Miscellaneous Publ., 256.
- [5] MIRANDA, H., CUMBRERA, F. L., CONDE, A., MARQUEZ, R., *Portgal. Phys.*, **13**, 53 (1982).
- [6] NABITOVICH, I. D., STETSIV, YA. I., VOLOSHCHUK, YA. V., *Sov. Phys. Cryst.*, **12**, 513 (1968).
- [7] BORN, M., WOLF, E., *Principles of Optics*. Pergamon Press Inc., p. 617 (1959).
- [8] DAVIS, E. A., MOTT, N. F., *Phil. Mag.*, **22**, 903 (1970).